

Published in final edited form as:

*Adv Drug Deliv Rev.* 2010 December 30; 62(15): 1530–1540. doi:10.1016/j.addr.2010.05.002.

## Multivalent protein polymers with controlled chemical and physical properties

Ayben Top and Kristi L. Kiick\*

Department of Materials Science and Engineering, 201 DuPont Hall, University of Delaware, Newark, Delaware 19716

### Abstract

In this review, we describe our work on the design, characterization, and modification of a series of alanine-rich helical polypeptides with novel functions. Glycosylation of the polypeptides has permitted investigation of polymer architecture effects on multivalent interactions. One of the members of this polypeptide family exhibits polymorphological behavior that is easily manipulated via simple changes in solution pH and temperature. Polypeptide-based fibrils formed at acidic pH and high temperature were shown to direct the one-dimensional organization of gold nanoparticles via electrostatic interactions. As a precursor to fibrils, aggregates likely comprising alanine-rich cores form at low temperatures and acidic pH and reversibly dissociate into monomers upon deprotonation. PEGylation of these polypeptides does not alter the self-association or conformational behavior of the polypeptide, suggesting potential applications in the development of assembled delivery vehicles, as modification of the polypeptides should be a useful strategy for controlling assembly.

### Keywords

Polypeptide; biosynthesis; self-assembly; fibril; multivalent interactions; nanostructure; PEGylation; glycopolymer; nanoparticle array

## 1. Introduction

Biosynthetic methods employ the precisely templated polymerization of proteins from their genes, and have yielded a wide variety of natural and artificial proteins. With fidelity superior to synthetic polymerization methods, nature's translation machines work in an almost error-free fashion to yield identical macromolecules. As has been widely described over the past decade and longer [1-5], biosynthetic methods thus afford polymers of precise structure, monomer sequence, and molecular mass [1-9]. At the genetic level, a range of synthetic controls are available; existing natural genes can be amplified from complementary deoxyribonucleic acid (cDNA) templates, repetitive sequences of naturally occurring genes can be multimerized to yield repetitive sequences of various molecular weights, or entirely de novo sequences can be engineered. Protein polymers modeled after the natural structural proteins silk [10-14], elastin [15-23], and collagen [24,25] have

© 2010 Elsevier B.V. All rights reserved.

\*to whom correspondence should be addressed. kiick@udel.edu, 302-831-0201(tel), 302-831-4545(fax).

**Publisher's Disclaimer:** This is a PDF file of an unedited manuscript that has been accepted for publication. As a service to our customers we are providing this early version of the manuscript. The manuscript will undergo copyediting, typesetting, and review of the resulting proof before it is published in its final citable form. Please note that during the production process errors may be discovered which could affect the content, and all legal disclaimers that apply to the journal pertain.

dominated this area, although de novo sequences have also become of increasing interest [6-9,26-28]. After production of the protein polymer, there are opportunities for subsequent chemical modification, control of folding, and modulation of assembly.

Biosynthetic methods also allow facile synthesis of multi-block polymers with desired number and composition of blocks, which has yielded a variety of materials including nanoparticles and responsive hydrogels; modulation of the properties of the molecules is afforded by alterations in composition [20,22,29-45]. For example, control of the composition of silk-elastin block polypeptides has yielded structures in which gelation and subsequent release of bioactive molecules can be tuned, emphasizing the crucial role of biosynthetic methods in the study of the structure-function relationships [30,43,46].

The controlled structure and inherent biocompatibility of many of these polymers, coupled with the facile incorporation of functional domains in these polypeptides, have provided enormous opportunities to create functional biomaterials. Cell-adhesion domains [20,31,35,37,39,42,47,48,49], enzymatic degradation sequences [39,42,49], ligand-binding sites [41,44,45,50], self-assembly triggers [22,29,30,32] and chemical modification sites [6-9,39,42,51-60] have all been included in modular polypeptide-based designs. Recently developed cationic polypeptides represent one such kind of functional material for gene transfection applications. In these constructs, multifunctional domains comprising a nucleic-acid-binding domain composed of predominantly basic amino acids, a targeting moiety (e.g., basic fibroblast growth factor (FGF2) ligands), a membrane disruption unit (e.g., transactivator of transcription (TAT) or other fusogenic peptides), and a nuclear localization signal facilitate delivery of genes from the matrix [41,44,45,61-63]. Extracellular matrix-mimetic polypeptides, engineered with biological cues, represent another type of functional biomaterial, with intended applications in tissue engineering and/or controlled release. The widely exploited, fibronectin-derived cell adhesive arginyl-glycyl-aspartate (RGD) peptide domain has been incorporated into a variety of protein-based polymers – based on silk [47-48], elastin [31,35,37,49] and resilin [42] – to regulate the cell-adhesive function of the materials. Elaboration of multiple biological functions is straightforward with biosynthetic approaches, and materials that contain additional domains, such as proteolytic degradation sites and heparin-binding domains have also been reported [39,42,49].

The incorporation of non-natural amino acid derivatives in genetically engineered polypeptides has yielded another approach to expand their functionality. Fluorine derivatives of aliphatic amino acids such as leucine, isoleucine, and valine, and the aromatic phenylalanine, impart hydrolytic, thermal, and chemical stability owing to the super-hydrophobicity of fluorine [64-70]. Polypeptides have also been equipped with novel chromophores and photoreactive residues via the incorporation of non-natural analogs or mimetics of aromatic amino acids [71-77], with reported applications in photopatterning [78] and photocrosslinking [79]. Furthermore, the incorporation of reactive non-natural amino acids such as those containing alkene [80-84], alkyne [85-87], azide [86-90] and ketone [91-92] groups, has provided unique opportunities to yield protein polymers with selective sites for orthogonal chemical modification.

The naturally occurring lysine, glutamic acid and cysteine residues, nevertheless, have remained a mainstay for chemical modification of protein-based polymers. Chemical crosslinking through these residues has been used to facilitate network formation of the artificial polypeptides as an alternative to self-assembly or to tune mechanical properties of the polypeptide films or hydrogels [9,20,42,51,53,58,60]. Chemical conjugation through these reactive groups also offers a wide spectrum of modifications spanning from PEGylation to attachment of small bioactive molecules, although PEGylation has not been as widely employed for modification of protein polymers as it has for modification of some

therapeutic proteins [93-98]. PEGylation has been exploited to control fibrillar assembly of the polypeptide [(AG)<sub>3</sub>EG]<sub>n</sub> (n = 10-20) by preventing stacking of β-sheet structures [54,56], as well as to crosslink biologically active recombinant polypeptides to yield *in situ* forming hydrogels [39]. Chemical conjugation has also permitted incorporation of cell-adhesion ligands such as cyclic RGD, which cannot be incorporated via genetic methods [59]. Smart multi-functional tumor-targeting drug delivery systems were developed by combining thermoresponsive behavior of elastin like polypeptides (ELPs) and chemical conjugation methods. The antitumor drug, doxorubicin, was attached to ELPs via reaction with lysine or cysteine residues, and the pH-programmed release of the drug was tuned by the nature of crosslinkers or by the incorporation of a peptide-based lysosomally degradable domain. The lower critical solution temperature (LCST) behavior of the ELPs was exploited to control the response of the ELPs to hyperthermic. The composition of the ELP was modulated such that its thermal transition temperature lies between body temperature and hyperthermic tumor temperature. Hence, above its transition temperature, self-association of ELP facilitated drug transport passively via the enhanced permeability retention (EPR) effect. Likewise, in multi-functional cationic drug delivery systems, active targeting to these ELPs was imparted by incorporation of specific cell-binding motifs, such as the TAT derived peptide, to ensure cellular uptake [52,55,57]. Similarly, we have recently demonstrated the production of well-defined, glycosylated random coil and alanine-rich helical polypeptides that inhibit cholera toxin via multivalent interactions [7,8,99,100]. These random coil and helical polypeptides, in which the spacing of the glutamic acid residues was manipulated via their genetically-directed placement in the chain, have been functionalized with *N*-(ε-aminocaproyl)-β-D-galactosylamine and other saccharides. Glycopolypeptides in which the inter-residue distance approximates the inter-receptor spacing of cholera toxin (~35-37 Å) showed significantly improved inhibition, yielding insights into the toxin-carbohydrate interactions and in the design of novel glycopolypeptides [8,100].

These helical polypeptides, equipped with chemically reactive glutamic acid residues, have provided a versatile platform not only for generating scaffolds that can modulate multivalent binding events, but also in the assembly of nanostructures with potential application in drug delivery and organization/immobilization of inorganic materials. In this review, we summarize our recent findings on the conformational and aggregation behavior of these polypeptides, along with our ongoing modification of these polypeptides – via glycosylation, attachment of gold nanoparticles and PEGylation – in the generation of novel protein-based, functional materials.

## 2. Alanine-rich helical polypeptides

In the design of the helical polypeptides, alanine, glutamine and glutamic acid residues were employed due to their high helical propensity [101]. Additionally, the polar amino acids glutamine and glutamic acid impart water solubility. The reactive glutamic acid was selected as a chemical modification site over lysine and cysteine because of the demonstrated facile expression and purification of polypeptides containing anionic amino acids [6]. These macromolecules were initially investigated as unique scaffolds in the generation of well-defined glycopolymers, and were accordingly chemically modified with amine-functionalized saccharides, to study multivalent carbohydrate-protein interactions. The glutamic acid residue spacing in the polypeptides was varied in a range of distances relevant to those exhibited between adjacent binding sites of toxins; the precise positions for the glutamic acid residues were suggested by energy minimization calculations. The resultant polypeptides, given in Table 1, were produced recombinantly employing *Escherichia coli* (*E. coli*) as the expression host. The sequences were equipped with an N-terminal decahistidine sequence to facilitate purification via nickel nitrilotriacetic acid (Ni-NTA)

affinity chromatography [6,7,102]. Seamless cloning and standard gene multimerization methods [16,103] were slightly modified to yield repetitive protein polymers with no extraneous amino acids. The representative simplified plasmid construction route used to generate the polypeptide 17-H-6 (Table 1) is provided in Figure 1. The expression of the polypeptides was conducted in cultures of *E. coli* strain BL21(DE3)plysS, with standard isopropyl- $\beta$ -D-thiogalactopyranoside (IPTG) induction, and the polypeptides were purified via immobilized metal affinity chromatography under denaturing conditions by applying pH and/or imidazole gradients. With optimization of purification conditions, it is possible to obtain 50-100 mg of polypeptide with greater than 90-95% purity; the purity of polypeptides was indicated in all cases by sodium dodecyl sulfate polyacrylamide gel electrophoresis (SDS-PAGE), high-performance liquid chromatography (HPLC), and amino acid analyses. The molecular masses of the polypeptides were confirmed by matrix-assisted laser desorption/ionization-time of flight (MALDI-TOF) mass spectrometry [6,7,102].

### 3. Properties under physiological conditions

Circular dichroic (CD) spectroscopy was used to provide experimental evidence of the helical conformation of all of the polypeptides delineated in Table 1; representative CD spectra of 17-H-3, 17-H-6, and 35-H-6 at physiological pH and isotonic conditions are shown in Figure 2. The polypeptides have an  $\alpha$ -helical conformation as indicated by the presence of the double minima at 208 and 222 nm in their spectra, corroborating energy minimization calculations. The percent helicity values of the polypeptides at 5 °C were estimated to be approximately 50%, 65%, and 70% for 17-H-3, 17-H-6 and 35-H-6 respectively [102]; the helicity of the polypeptides increases with increasing molecular weight as expected [104]. Slight difference in the helicities of 35-H-6 and 17-H-6 can be attributed to the stabilization of the helix by interactions between glutamic acid and glutamine at *i* and *i*+4 positions [105]; helix-destabilizing repulsions between glutamic acid residues are eliminated under the conditions of the CD experiments (150 mM NaCl) as the Debye length under these conditions (7.8 Å) is significantly lower than the distance between glutamic acids (17 Å and 35 Å) [106].

To provide deeper insight into the conformational stability and potential association of these sequences, temperature-induced conformational changes were monitored for 17-H-6 (in phosphate buffered saline (PBS) at pH 7.4) via CD spectroscopy; the polypeptides convert from an alpha-helical to a non-helical conformation upon heating. The reversibility of the thermal denaturation was indicated by the lack of change observed in the mean residue ellipticity values prior to unfolding and after refolding (Figure 3), as well as by the overlap of consecutive scans in differential scanning calorimetry experiments [107].

The aggregation state of the polypeptides offers a key variable for their potential application, as self-assembly of the polypeptides provides a desirable bottom-up approach to prepare nanostructures but is undesirable in the controlled presentation of multivalent ligands. A lack of aggregation in these sequences under neutral pH and isotonic salt conditions was confirmed by sedimentation equilibrium experiments, in which the differences between theoretical and experimental molecular weight values were lower than 10%, indicating the polypeptides (17-H-3, 17-H-6, and 35-H-6) are monomeric at low concentrations. Native gel electrophoresis confirmed the lack of aggregation of the polypeptides at higher concentrations (Figure 4), with no change in molecular mass indicated at concentrations higher than 100  $\mu$ M [102]. The absence of self-association for the polypeptide with the highest glutamic acid density, 17-H-6, was also confirmed by the overlap of CD melting curves of the polypeptide at different concentrations [107]. Altogether, the data confirm that the polypeptide scaffolds are monomeric at physiological pH and isotonic conditions, suggesting their value in the study of multivalent interactions.

#### 4. Glycosylated helical polypeptide scaffolds

The number and spacing of ligands and the size of a polymeric scaffold are important parameters in scaffolds that mediate multivalent interactions [108-111]. However, the effects of scaffold conformation were not investigated in detail prior to our production of glycopolypeptides with various backbone architectures. In order to elucidate the effect of backbone conformation on multivalent binding events, glycosylated scaffolds of both random-coil and alpha-helical conformation were produced for inhibition of the binding of the B<sub>5</sub> subunit of the cholera toxin. Glycosylation was achieved via the reaction between amine groups of *N*-( $\epsilon$ -aminocaproyl)- $\beta$ -D-galactosylamine) and carboxyl groups of glutamic acid residues as mentioned above. Nearly quantitative functionalization of the polypeptides was confirmed via proton nuclear magnetic resonance (<sup>1</sup>H NMR) spectroscopy, SDS-PAGE analysis, and spectrophotometric evaluation of saccharide content. CD spectra of the glycosylated helical scaffolds (17-H-3, 17-H-6, and 35-H-6) showed that the polypeptides retain their alpha-helical conformation upon glycosylation. An enzyme-linked assay of cholera toxin inhibition yielded dose-response curves for the inhibition by these different glycopolypeptides, which are shown in Figure 5. Half maximal inhibitory concentration (IC<sub>50</sub>) values from the non-linear fit to inhibition curves were obtained as 55 mM, 3.34 mM, 725  $\mu$ M and 160  $\mu$ M for monovalent galactose, and glycosylated polypeptides denoted as Cap 17-H-3, Cap 17-H-6 and Cap 35-H-6, respectively, clearly suggesting the effects of multivalency, molecular weight, and saccharide spacing on inhibition [100]. Most importantly, the enhanced inhibitory effect of the Cap 35-H-6, the glycopolypeptide with lower valency but saccharide spacing that matches the adjacent binding sites of cholera toxin, confirms the important role of saccharide spacing in improving inhibitory potential in these classes of molecules, consistent with the findings of random-coil glycopolypeptides [8,100].

Comparison of inhibition improvement values of genetically engineered random coil (RC) glycopolypeptides and glycosylated polyglutamates at different molecular weights indicated that the hydrodynamic volume of the glycopolypeptide (expressed as retention time in a gel permeation chromatography (GPC) experiment), rather than the molecular mass alone, plays a key role in inhibition. A slight improvement in the inhibitory potential of the Cap 35-RC-6 (glycosylated random coil analogue of 35-H-6) glycopolypeptide, over that anticipated based on its hydrodynamic volume, was observed [8]. Shorter, modified RC scaffolds that exhibit similar hydrodynamic volumes as 35-RC-6 exhibit improved inhibition, confirming the role of hydrodynamic volume and guiding the design of new multivalent inhibitors. As shown in Figure 6, however, the helical Cap 35-H-6 exhibits the greatest inhibition improvement. These findings corroborate the role of appropriate spacing, and also underscore that scaffold rigidity plays a key role in improving inhibition, likely through a reduction in conformational entropy loss upon binding [8,100]. The opportunities to control ligand spacing, scaffold size and architecture effects in these macromolecules, coupled with their improved binding of cholera toxin, suggests that these genetically engineered, polypeptide-based scaffolds offer a reliable model system in investigating multivalent events.

#### 5. Controlled aggregation of alanine-rich polypeptides

In addition to our interest in multivalent binding by the helical polypeptides, we speculated that the protonation of the glutamic acid residues in these sequences would afford facile opportunities to manipulate their folding and assembly behavior. Characterization by CD spectroscopy, at acidic pH, of the polypeptides 17-H-3, 17-H-6, and 35-H-6 indicated that all showed helical secondary structure under these conditions, with helicity values similar to those observed at pH 7.4 [7,107]. Detailed characterization of the helical polypeptide of



highest glutamic density, 17-H-6, was conducted at acidic pH to complement the data presented above for the polypeptide under neutral conditions. Interestingly, under these conditions (low pH, isotonic salt), the concentration-dependent, thermal melting curves observed in CD showed shifts in the melting temperature of the polypeptides with increasing polypeptide concentration, suggesting self-association. The sizes of the aggregates were determined via dynamic light scattering under these solution conditions at 20 °C. The hydrodynamic radii of the polypeptide aggregates were indicated to be approximately ~10-20 nm, depending on the concentration of the polypeptide and solution temperature. The scattering of the aggregates via light scattering was characterized upon the cycling of pH between 2.3 and 7.4, with an increase in intensity taken as an indicator of aggregate formation. As shown in Figure 7, comparison of the scattering intensities of the polypeptide at acidic and neutral pH indicated that the association of the polypeptides is facilitated at low pH and is immediately and reversibly responsive to changes in pH. The aggregation number of these structures was estimated to be around a few hundred macromolecules, as suggested via a combination of sedimentation velocity and DLS data [107]. More detailed characterization of the morphologies of the aggregates in solution via cryo-TEM indicates an elongated morphology (with an average width of ~10 nm and average length of ~50 nm) for these structures (unpublished data), which may be exploited in future application.

The association of the helical polypeptides might also promote larger-scale aggregation into other morphologies. Thus thermal denaturation, which has been shown to promote fibril formation for other proteins [112-116], was exploited to test the range of morphologies possible from the alanine-rich polypeptides. First, variations in polypeptide conformation as a function of temperature were monitored via CD. In refolding experiments, some loss of helicity in the polypeptide was observed (Figure 8), likely due to the irreversible formation of non-helical structures. The possibility that these structures were  $\beta$ -sheet suggested interesting opportunities for fibril formation and functionalization. Although observation of  $\beta$ -sheet structure formed at early stages was obscured by the strong random coil signal in the CD spectrum at elevated temperatures, it became detectable upon prolonged incubation (ca. 7.5 hrs at 80 °C). Corroborating this CD data, the differential scanning calorimetry (DSC) data for 17-H-6 showed an exotherm at high temperatures, suggesting precipitation or aggregation of the polypeptide; the lack of overlap in consecutive DSC scans clearly indicated that this transition is irreversible (Figure 9). Characterization, by TEM, of the structures formed at high temperature unambiguously showed their fibrillar nature, as expected for  $\beta$ -sheet-forming peptides and proteins, with fibrils approximately 7 nm in width (Figure 10).

In summary, the aggregation tendency and resultant (nano)structures of the 17-H-6 polypeptide can be easily modulated by simple alterations in pH and temperature; the overall schematic illustrating the pathways for these transitions is shown in Figure 11. At low temperature and at neutral pH, when glutamic acid residues are charged, 17-H-6 forms a monomeric alpha-helical structure. However, reduction of the pH (to below the  $pK_a$  of glutamic acid) eliminates electrostatic repulsion, and the polypeptide reversibly forms structures comprising multiple macromolecules with alpha-helical conformation at low temperature. It is likely that this aggregate formation is mediated by the hydrophobic association of the alanine-rich domains and that the aggregates are stabilized by the positive charge of the N-terminal histidine tag of these sequences. (When the N-terminal decahistidine sequence is removed by cyanogen bromide (CNBr) mediated cleavage, the polypeptide becomes insoluble at pH 2.3.) Upon an increase in temperature, the polypeptide reversibly unfolds/refolds at neutral pH. However, at acidic pH, the polypeptide forms fibrillar  $\beta$ -sheet structures upon incubation at elevated temperatures; our current experimental data suggest that the initial formation of the multi-macromolecular aggregates accelerates the formation of  $\beta$ -sheet structure [107]. The polypeptide thus provides

macromolecular assemblies with morphologies that can be modulated with simple external stimuli, pH and temperature. Coupled with its uniform and controlled chemical structure, this suggests its potential in nanotechnology applications.

## 6. Fibril-directed gold nanoparticle organization

The detailed assembly and structure of the fibrils was provided by wide angle X-ray scattering (WAXS), Fourier transform infra-red (FTIR) spectroscopy, atomic force microscopy (AFM) and optical microscopy techniques (Figure 12) [117]. In X-ray scattering, a broad peak corresponding to a d-spacing of 4.56 Å was obtained, consistent with the hydrogen-bonding distance between  $\beta$ -sheet strands in peptides and proteins [118,119]. Characterization by FTIR spectroscopy also confirmed the  $\beta$ -sheet conformation of the fibrils, with peaks corresponding to those expected for  $\beta$ -sheet strands ( $1624\text{ cm}^{-1}$ ) and antiparallel  $\beta$ -sheet structure ( $1690\text{ cm}^{-1}$ ) [120]. The fibrils showed green colored birefringence, upon staining with Congo red, in optical microscopy under cross-polarizers, suggesting a cross- $\beta$ -sheet structure for the fibrils, i.e.  $\beta$ -strands are perpendicular to the fibrillar growth. The fact that these fibrils bound thioflavin T furthered confirmed this model [121,122]. From high-resolution TEM images, the fibril width was measured as  $7.6 \pm 0.4$  nm, consistent with the length of the 22-amino-acid repeat unit of the 17-H-6 (Table 1) in a  $\beta$ -sheet conformation (ca. 7.7 nm). In AFM, the height of the fibrils was measured in discrete steps of  $1.4 \pm 0.1$ ,  $2.8 \pm 0.1$ , and  $4.0 \pm 0.1$  nm, suggesting a rectangular rather than cylindrical structure. These findings suggest that the polypeptide adopts a folded antiparallel  $\beta$ -sheet conformation, with a width corresponding to a single repeat unit of the alanine-rich domain, to form a cross- $\beta$ -sheet fibril with an inter-strand d-spacing of 4.56 nm. It is likely that the axial growth of the fibrils occurs by the addition of folded chains in a head-to tail fashion, which (1) permits burial of the C-terminal ends of the chains to maximize hydrophobic contacts and (2) would place the N-terminal histidine tags adjacent to one other as proposed in Figure 12. The hydrogen bonding and hydrophobic contacts must dominate the assembly, with electrostatic repulsion between histidine segments contributing only marginally to the opposition of the assembly. The histidine-rich segment is thus arranged regularly along the fibril length with a spatial periodicity of ca. 5.5 nm ( $12 \times 4.56\text{Å}$ ).

These regularly repeating, positively charged histidine patches represent the most promising feature of this nano-architecture, as they can be utilized for the controlled placement of oppositely charged inorganic nanoparticles. To demonstrate the possibility for electrostatically controlled, one-dimensional assembly of inorganic nanoparticles, preformed 17-H-6 fibrils were mixed together with an excess of negatively charged gold nanoparticles (formed via citrate-reduction methodologies [123]). With overnight stirring, the gold nanoparticles are immobilized on the 17-H-6 fibrils, thus neutralizing the charge on the positively charged histidine patches, and the fibril-particle assemblies precipitate from solution. Characterization of the fibril-particle assemblies via bright-field TEM (BF-TEM; Figure 13) clearly illustrates that the gold nanoparticles are controllably immobilized on the fibrils, with successful templating over distances of hundreds of nanometers. Statistical analysis of the inter-nanoparticle spacing of the BF-TEM images yields inter-particle distances of  $5.5 \pm 1.2$  nm, in excellent agreement with the model proposed in Figure 12 [117]. That this assembly is templated and not merely a result of electrostatically mediated deposition of the nanoparticles on a uniformly charged fibril is suggested by Debye theory. The particles are not close-packed, nor is the interparticle distance dictated by the Debye length of the solution.

The modularity of these polypeptides is a key design advantage, and suggests numerous opportunities to engineer assemblies via the modulation of fusion tags and particle surfaces. The polypeptide assembly also offers a convenient method for bottom up placement of

nanoparticles at predefined separations and at length scales which are at the limit of state-of-the-art lithographic capabilities. Variations in the distance between nanoparticles should be easily accessible via variations in the number of repeats of the alanine-rich domains, and versatility in the types of nanoparticles immobilized can be obtained via straightforward engineering of the fusion tags on the polypeptide. Such one dimensional particle displays would be useful for optoelectronic devices and biomaterials systems, and the elaboration of two and three-dimensional displays is under investigation.

## 7. Ongoing work

The flexibility of the assembly of these polypeptides, coupled with their potential use as multivalent pharmaceuticals and/or multivalent displays of small molecule drugs and ligands, has motivated additional studies of their PEGylation and self-assembly. The PEGylation of 17-H-6 has provided useful information on the conformation, thermal stability, aggregation, and fibrillization behavior of the polypeptide, and similar polypeptide-based systems have potential application in the development of PEGylated polypeptide-drug conjugates.

In order to prepare mono-PEGylated 17-H-6 conjugates, the N-terminal histidine tag of the polypeptide was removed via cleavage by CNBr, followed by reaction of the polypeptide with propionaldehyde-functionalized methoxypoly(ethylene glycol) (mPEG) (5KDa or 10 KDa) with the N-terminal amine of the cleaved polypeptide. The monoPEGylated conjugate was isolated using anion exchange and size exclusion chromatography and its formation was confirmed by MALDI-TOF mass spectroscopy. CD characterization of the conjugates has shown that the N-terminal mono-PEGylation has no impact on the conformation or conformational changes of the polypeptide, but retards  $\beta$ -sheet formation at low pH. TEM characterization of the conjugates (after incubation at 80 °C at pH 2.3 for 18 hours) indicates that the polypeptides are no longer competent for the formation of uniform fibrils; only non-uniform fibrils of greater widths were observed (unpublished data). These data confirm that PEGylation interferes with the fibrillization of the polypeptide, as anticipated based on other studies of PEGylated,  $\beta$ -sheet-forming peptides and polypeptides [54,56,124,125], although the details of this interference have not yet been elucidated for the 17-H-6-based fibrils.

Our initial structural characterization of the conjugates has also indicated that they retain their pH responsiveness, and form similar, although slightly smaller, structures as those formed by non-PEGylated 17-H-6 at low pH. The detailed characterization of 17-H-6, coupled with these initial investigations of the PEGylated version of the polypeptide, indicates that self-assembly triggered by protonation of glutamic acid residues is operative in both cases (unpublished data). Therefore, the development of polypeptide-based micellar delivery vehicles, in which hydrophobic drugs are conjugated to the glutamic acid residues of these sequences [126-128] or in which a therapeutic multivalent polypeptide serves as the associating domain, should be possible. Variations in the assembled structures of these conjugates, and their potential selectivity based on their architecture, will offer interesting drug carrier systems in which rates of release, biodistribution, and cellular uptake may all be modulated [129-131].

## 8. Conclusions

We have synthesized a series of helical polypeptides using biosynthetic methods and characterized in detail their conformational and assembly properties. These macromolecules have been shown to be versatile scaffolds, with many applications including in the production of multivalent ligands, controlled immobilization of nanoparticles, and assembled structures. Their properties and assembly are easily manipulated via simple



stimuli such as solution pH and temperature, and their assembly occurs under benign conditions that will facilitate their application in the biological environment. Enormous opportunities exist for creating functional materials based on these genetically engineered polypeptides, via exploitation of their defined structures and their chemical modification. Development of rules relating their structure to their conformation and sequence will facilitate the rational design and expansion of their functionality.

## Acknowledgments

The authors' work in these areas has been funded by grants from the National Institutes of Health (1-RO1-EB006006), the National Science Foundation (DMR 0210223), and the National Aeronautics and Space Administration (NA68-01923). Facilities and other support have also come from the National Center for Research Resources, a division of the National Institutes of Health (1-P20-RR017716). Its contents are the sole responsibility of the authors and do not necessarily represent the official views of the NCRR or NIH.

## References

- [1]. Cappello J, Crissman J, Dorman M, Mikolajczak M, Textor G, Marquet M, Ferrari F. Genetic-engineering of structural protein polymers. *Biotechnol. Progr.* 1990; 6:198–202.
- [2]. Ghandehari H, Cappello J. Genetic engineering of protein-based polymers: Potential in controlled drug delivery. *Pharm. Res.* 1998; 15:813–815. [PubMed: 9647343]
- [3]. van Hest JCM, Tirrell DA. Protein-based materials, toward a new level of structural control. *Chem. Commun.* 2001; 19:1897–1904.
- [4]. Kiick KL. Biosynthetic methods for the production of advanced protein-based materials. *Polym. Rev.* 2007; 47:1–7.
- [5]. Farmer, RS.; Charati, MB.; Kiick, KL. Biosynthesis of protein-based polymeric materials. In: Matyjaszewski, K.; Gnanou, Y.; Leibler, L., editors. *Macromolecular Engineering: Precise Synthesis, Materials Properties, Applications*. Vol. 1. Wiley; Weinheim: 2007. p. 479-518.
- [6]. Farmer RS, Kiick KL. Conformational behavior of chemically reactive alanine-rich repetitive protein polymers. *Biomacromolecules.* 2005; 6:1531–1539. [PubMed: 15877375]
- [7]. Farmer RS, Argust LM, Sharp JD, Kiick KL. Conformational properties of helical protein polymers with varying densities of chemically reactive groups. *Macromolecules.* 2006; 39:162–170. [PubMed: 19180254]
- [8]. Polizzotti BD, Maheshwari R, Vinkenburg J, Kiick KL. Effects of saccharide spacing and chain extension on toxin inhibition by glycopolypeptides of well-defined architecture. *Macromolecules.* 2007; 40:7103–7110. [PubMed: 19169374]
- [9]. Davis NE, Karfeld-Sulzer LS, Ding S, Barron AE. Synthesis and characterization of a new class of cationic protein polymers for multivalent display and biomaterial applications. *Biomacromolecules.* 2009; 10:1125–1134. [PubMed: 19361214]
- [10]. Prince JT, McGrath KP, Digirolamo CM, Kaplan DL. Construction, cloning, and expression of synthetic genes encoding spider dragline silk. *Biochemistry.* 1995; 34:10879–10885. [PubMed: 7662669]
- [11]. Arcidiacono S, Mello C, Kaplan D, Cheley S, Bayley H. Purification and characterization of recombinant spider silk expressed in *Escherichia coli*. *Appl. Microbiol. Biot.* 1998; 49:31–38.
- [12]. Winkler S, Szela S, Avtges P, Valluzzi R, Kirschner DA, Kaplan D. Designing recombinant spider silk proteins to control assembly. *Int. J. Biol. Macromol.* 1999; 24:265–270. [PubMed: 10342773]
- [13]. Szela S, Avtges P, Valluzzi R, Winkler S, Wilson D, Kirschner D, Kaplan DL. Reduction-oxidation control of  $\beta$ -sheet assembly in genetically engineered silk. *Biomacromolecules.* 2000; 1:534–542. [PubMed: 11710178]
- [14]. Zhou YT, Wu SX, Conticello VP. Genetically directed synthesis and spectroscopic analysis of a protein polymer derived from a flagelliform silk sequence. *Biomacromolecules.* 2001; 2:111–125. [PubMed: 11749162]

- [15]. McPherson DT, Morrow C, Minehan DS, Wu JG, Hunter E, Urry DW. Production and purification of a recombinant elastomeric polypeptide, G-(VPGVG)<sub>19</sub> VPGV, from *Escherichia coli*. *Biotechnol. Progr.* 1992; 8:347–352.
- [16]. McMillan RA, Lee TAT, Conticello VP. Rapid assembly of synthetic genes encoding protein polymers. *Macromolecules.* 1999; 32:3643–3648.
- [17]. Huang L, McMillan RA, Apkarian RP, Pourdeyhimi B, Conticello VP, Chaikof EL. Generation of synthetic elastin-mimetic small diameter fibers and fiber networks. *Macromolecules.* 2000; 33:2989–2997.
- [18]. McMillan RA, Conticello VP. Synthesis and characterization of elastinmimetic protein gels derived from a well-defined polypeptide precursor. *Macromolecules.* 2000; 33:4809–4821.
- [19]. Lee TAT, Cooper A, Apkarian RP, Conticello VP. Thermo-reversible self assembly of nanoparticles derived from elastin-mimetic polypeptides. *Adv. Mater.* 2000; 12:1105–1110.
- [20]. Welsh ER, Tirrell DA. Engineering the extracellular matrix: A novel approach to polymeric biomaterials. I. Control of the physical properties of artificial protein matrices designed to support adhesion of vascular endothelial cells. *Biomacromolecules.* 2000; 1:23–30. [PubMed: 11709838]
- [21]. Meyer DE, Shin BC, Kong GA, Dewhirst MW, Chilkoti A. Drug targeting using thermally responsive polymers and local hyperthermia. *J. Control. Release.* 2001; 74:213–224. [PubMed: 11489497]
- [22]. Wright ER, McMillan RA, Cooper A, Apkarian RP, Conticello VP. Thermoplastic elastomer hydrogels via self-assembly of an elastin-mimetic triblock polypeptide. *Adv. Funct. Mater.* 2002; 12:149–154.
- [23]. Meyer DE, Chilkoti A. Genetically encoded synthesis of protein-based polymers with precisely specified molecular weight and sequence by recursive directional ligation: Examples from the elastin-like polypeptide system. *Biomacromolecules.* 2002; 3:357–367. [PubMed: 11888323]
- [24]. Frank S, Kammerer RA, Mechling D, Schulthess T, Landwehr R, Bann J, Guo Y, Lustig A, Bachinger HP, Engel J. Stabilization of short collagen-like triple helices by protein engineering. *J. Mol. Biol.* 2001; 308:1081–1089. [PubMed: 11352592]
- [25]. Boudko S, Frank S, Kammerer RA, Stetefeld J, Schulthess T, Landwehr R, Lustig A, Bachinger HP, Engel J. Nucleation and propagation of the collagen triple helix in single-chain and trimerized peptides: Transition from third to first order kinetics. *J. Mol. Biol.* 2002; 317:459–470. [PubMed: 11922677]
- [26]. McGrath KP, Fournier MJ, Mason TL, Tirrell DA. Genetically directed syntheses of new polymeric materials. Expression of artificial genes encoding proteins with repeating (AlaGly)<sub>3</sub>ProGluGly elements. *J. Am. Chem. Soc.* 1992; 114:727–733.
- [27]. Krejchi MT, Atkins EDT, Waddon AJ, Fournier MJ, Mason TL, Tirrell DA. Chemical sequence control of  $\beta$ -sheet assembly in macromolecular crystals of periodic polypeptides. *Science.* 1994; 265:1427–1432. [PubMed: 8073284]
- [28]. Topilina NI, Higashiya S, Rana N, Ermolenkov VV, Kossow C, Carlsen A, Ngo SC, Wells CC, Eisenbraun ET, Dunn KA, Lednev IK, Geer RE, Kaloyeros AE, Welch JT. Bilayer fibril formation by genetically engineered polypeptides: Preparation and characterization. *Biomacromolecules.* 2006; 7:1104–1111. [PubMed: 16602727]
- [29]. Petka WA, Harden JL, McGrath KP, Wirtz D, Tirrell DA. Reversible hydrogels from self-assembling artificial proteins. *Science.* 1998; 281:389–392. [PubMed: 9665877]
- [30]. Cappello J, Crissman JW, Crissman M, Ferrari FA, Textor G, Wallis O, Whitley JR, Zhou X, Burman D, Aukerman L, Stedronsky ER. In-situ self-assembling protein polymer gel systems for administration, delivery, and release of drugs. *J. Control. Release.* 1998; 53:105–117. [PubMed: 9741918]
- [31]. Panitch A, Yamaoka T, Fournier MJ, Mason TL, Tirrell DA. Design and biosynthesis of elastin-like artificial extracellular matrix proteins containing periodically spaced fibronectin CS5 domains. *Macromolecules.* 1999; 32:1701–1703.
- [32]. Qu Y, Payne SC, Apkarian RP, Conticello VP. Self-assembly of a polypeptide multi-block copolymer modeled on dragline silk proteins. *J. Am. Chem. Soc.* 2000; 122:5014–5015.

- [33]. Megeed Z, Cappello J, Ghandehari H. Controlled release of plasmid DNA from a genetically engineered silk-elastinlike hydrogel. *Pharm. Res.* 2002; 19:954–959. [PubMed: 12180547]
- [34]. Nagarsekar A, Crissman J, Crissman M, Ferrari F, Cappello J, Ghandehari H. Genetic synthesis and characterization of pH- and temperature-sensitive silk-elastinlike protein block copolymers. *J. Biomed. Mater. Res.* 2002; 62:195–203. [PubMed: 12209939]
- [35]. Heilshorn SC, DiZio KA, Welsh ER, Tirrell DA. Endothelial cell adhesion to the fibronectin CS5 domain in artificial extracellular matrix proteins. *Biomaterials.* 2003; 24:4245–4252. [PubMed: 12853256]
- [36]. Yao JM, Asakura T. Synthesis and structural characterization of silk-like materials incorporated with an elastic motif. *J. Biochem.* 2003; 133:147–154. [PubMed: 12761210]
- [37]. Liu JC, Heilshorn SC, Tirrell DA. Comparative cell response to artificial extracellular matrix proteins containing the RGD and CS5 cell-binding domains. *Biomacromolecules.* 2004; 5:497–504. [PubMed: 15003012]
- [38]. Haider M, Leung V, Ferrari F, Crissman J, Powell J, Cappello J, Ghandehari H. Molecular engineering of silk-elastinlike polymers for matrix-mediated gene delivery: Biosynthesis and characterization. *Mol. Pharmaceut.* 2005; 2:139–150.
- [39]. Rizzi SC, Hubbell JA. Recombinant protein-co-PEG networks as cell-adhesive and proteolytically degradable hydrogel matrixes. Part 1: Development and physicochemical characteristics. *Biomacromolecules.* 2005; 6:1226–1238. [PubMed: 15877337]
- [40]. Sallach RE, Wei M, Biswas N, Conticello VP, Lecommandoux S, Dluhy RA, Chaikof EL. Micelle density regulated by a reversible switch of protein secondary structure. *J. Am. Chem. Soc.* 2006; 128:12014–12019. [PubMed: 16953644]
- [41]. Canine BF, Wang YH, Hatefi A. Biosynthesis and characterization of a novel genetically engineered polymer for targeted gene transfer to cancer cells. *J. Control. Release.* 2009; 138:188–196. [PubMed: 19379785]
- [42]. Charati MB, Ifkovits JL, Burdick JA, Linhardt JG, Kiick KL. Hydrophilic elastomeric biomaterials based on resilin-like polypeptides. *Soft Matter.* 2009; 5:3412–3416. [PubMed: 20543970]
- [43]. Dandu R, Von Cresce A, Briber R, Dowell P, Cappello J, Ghandehari H. Silk elastinlike protein polymer hydrogels: Influence of monomer sequence on physicochemical properties. *Polymer.* 2009; 50:366–374.
- [44]. Mangipudi SS, Canine BF, Wang YH, Hatefi A. Development of a genetically engineered biomimetic vector for targeted gene transfer to breast cancer cells. *Mol. Pharmaceut.* 2009; 6:1100–1109.
- [45]. Wang YH, Mangipudi SS, Canine BF, Hatefi A. A designer biomimetic vector with a chimeric architecture for targeted gene transfer. *J. Control. Release.* 2009; 137:46–53. [PubMed: 19303038]
- [46]. Hwang D, Moolchandani V, Dandu R, Haider M, Cappello J, Ghandehari H. Influence of polymer structure and biodegradation on DNA release from silk-elastinlike protein polymer hydrogels. *Int. J. Pharm.* 2009; 368:215–219. [PubMed: 19027056]
- [47]. Asakura T, Tanaka C, Yang MY, Yao JM, Kurokawa M. Production and characterization of a silk-like hybrid protein, based on the polyalanine region of *Samia cynthia ricini* silk fibroin and a cell adhesive region derived from fibronectin. *Biomaterials.* 2004; 25:617–624. [PubMed: 14607499]
- [48]. Tanaka C, Asakura T. Synthesis and characterization of cell-adhesive silk-like proteins constructed from the sequences of *Anaphe* silk fibroin and fibronectin. *Biomacromolecules.* 2009; 10:923–928. [PubMed: 19236090]
- [49]. Straley KS, Heilshorn SC. Independent tuning of multiple biomaterial properties using protein engineering. *Soft Matter.* 2009; 5:114–124.
- [50]. Hatefi A, Megeed Z, Ghandehari H. Recombinant polymer-protein fusion: a promising approach towards efficient and targeted gene delivery. *J. Gene Med.* 2006; 8:468–476. [PubMed: 16416505]
- [51]. Di Zio K, Tirrell DA. Mechanical properties of artificial protein matrices engineered for control of cell and tissue behavior. *Macromolecules.* 2003; 36:1553–1558.

- [52]. Dreher MR, Raucher D, Balu N, Colvin OM, Ludeman SM, Chilkoti A. Evaluation of an elastin-like polypeptide-doxorubicin conjugate for cancer therapy. *J. Control. Release.* 2003; 91:31–43. [PubMed: 12932635]
- [53]. Nowatzki PJ, Tirrell DA. Physical properties of artificial extracellular matrix protein films prepared by isocyanate crosslinking. *Biomaterials.* 2004; 25:1261–1267. [PubMed: 14643600]
- [54]. Smeenk JM, Otten MJB, Thies J, Tirrell DA, Stunnenberg HG, van Hest JCM. Controlled assembly of macromolecular  $\beta$ -sheet fibrils. *Angew. Chem. Int. Edit.* 2005; 44:1968–1971.
- [55]. Furgeson DY, Dreher MR, Chilkoti A. Structural optimization of a “smart” doxorubicin-polypeptide conjugate for thermally targeted delivery to solid tumors. *J. Control. Release.* 2006; 110:362–369. [PubMed: 16303202]
- [56]. Smeenk JM, Schon P, Otten MJB, Speller S, Stunnenberg HG, van Hest JCM. Fibril formation by triblock copolymers of silklike  $\beta$ -sheet polypeptides and poly(ethylene glycol). *Macromolecules.* 2006; 39:2989–2997.
- [57]. Bidwell GL, Fokt I, Priebe W, Raucher D. Development of elastin-like polypeptide for thermally targeted delivery of doxorubicin. *Biochem. Pharmacol.* 2007; 73:620–631. [PubMed: 17161827]
- [58]. Lim DW, Nettles DL, Setton LA, Chilkoti A. Rapid cross-linking of elastinlike polypeptides with (hydroxymethyl)phosphines in aqueous solution. *Biomacromolecules.* 2007; 8:1463–1470. [PubMed: 17411091]
- [59]. Kaufmann D, Fiedler A, Junger A, Auernheimer J, Kessler H, Weberskirch R. Chemical conjugation of linear and cyclic RGD moieties to a recombinant elastinmimetic polypeptide A versatile approach towards bioactive protein hydrogels. *Macromolecular Bioscience.* 2008; 8:577–588. [PubMed: 18350537]
- [60]. Lim DW, Nettles DL, Setton LA, Chilkoti A. In situ cross-linking of elastin like polypeptide block copolymers for tissue repair. *Biomacromolecules.* 2008; 9:222–230. [PubMed: 18163573]
- [61]. Rajagopalan R, Xavier J, Rangaraj N, Rao NM, Gopal V. Recombinant fusion proteins TAT-Mu, Mu and Mu-Mu mediate efficient non-viral gene delivery. *J. Gene Med.* 2007; 9:275–286. [PubMed: 17397090]
- [62]. Gao S, Simon MJ, Morrison B, Banta S. Bifunctional chimeric fusion proteins engineered for DNA delivery: Optimization of the protein to DNA ratio. *BBA-Gen. Subjects.* 2009; 1790:198–207.
- [63]. Xavier J, Singh S, Dean DA, Rao NM, Gopal V. Designed multi-domain protein as a carrier of nucleic acids into cells. *J. Control. Release.* 2009; 133:154–160. [PubMed: 18940210]
- [64]. Yoshikawa E, Fournier MJ, Mason TL, Tirrell DA. Genetically-engineered fluoropolymers. Synthesis of repetitive polypeptides containing p-fluorophenylalanine residues. *Macromolecules.* 1994; 27:5471–5475.
- [65]. Tang Y, Tirrell DA. Biosynthesis of a highly stable coiled-coil protein containing hexafluoroleucine in an engineered bacterial host. *J. Am. Chem. Soc.* 2001; 123:11089–11090. [PubMed: 11686725]
- [66]. Tang Y, Ghirlanda G, Petka WA, Nakajima T, DeGrado WF, Tirrell DA. Fluorinated coiled-coil proteins prepared in vivo display enhanced thermal and chemical stability. *Angew. Chem. Int. Edit.* 2001; 40:1494–1496.
- [67]. Tang Y, Ghirlanda G, Vaidehi N, Kua J, Mainz DT, Goddard WA, DeGrado WF, Tirrell DA. Stabilization of coiled-coil peptide domains by introduction of trifluoroleucine. *Biochemistry.* 2001; 40:2790–2796. [PubMed: 11258889]
- [68]. Lee KH, Lee HY, Slutsky MM, Anderson JT, Marsh ENG. Fluorous effect in proteins: De novo design and characterization of a four-alpha-helix bundle protein containing hexafluoroleucine. *Biochemistry.* 2004; 43:16277–16284. [PubMed: 15610021]
- [69]. Son S, Tanrikulu IC, Tirrell DA. Stabilization of *bzip* peptides through incorporation of fluorinated aliphatic residues. *Chembiochem.* 2006; 7:1251–1257. [PubMed: 16758500]
- [70]. Montclare JK, Son S, Clark GA, Kumar K, Tirrell DA. Biosynthesis and stability of coiled-coil peptides containing (2S,4R)-5,5,5-trifluoroleucine and (2S,4S)-5,5,5-trifluoroleucine. *Chembiochem.* 2009; 10:84–86. [PubMed: 19090517]

- [71]. Budisa N, Alefelder S, Bae JH, Golbik R, Minks C, Huber R, Moroder L. Proteins with  $\beta$ -(thienopyrrolyl)alanines as alternative chromophores and pharmaceutically active amino acids. *Protein Sci.* 2001; 10:1281–1292. [PubMed: 11420430]
- [72]. Budisa N, Rubini M, Bae JH, Weyher E, Wenger W, Golbik R, Huber R, Moroder L. Global replacement of tryptophan with aminotryptophans generates non invasive protein-based optical pH sensors. *Angew. Chem. Int. Edit.* 2002; 41:4066–4069.
- [73]. Kirshenbaum K, Carrico IS, Tirrell DA. Biosynthesis of proteins incorporating a versatile set of phenylalanine analogues. *Chembiochem.* 2002; 3:235–237. [PubMed: 11921403]
- [74]. Chin JW, Martin AB, King DS, Wang L, Schultz PG. Addition of a photocrosslinking amino acid to the genetic code of *Escherichia coli*. *P. Natl. Acad. Sci. U.S.A.* 2002; 99:11020–11024.
- [75]. Chin JW, Santoro SW, Martin AB, King DS, Wang L, Schultz PG. Addition of p-azido-L-phenylalanine to the genetic code of *Escherichia coli*. *J. Am. Chem. Soc.* 2002; 124:9026–9027. [PubMed: 12148987]
- [76]. Kwon I, Tirrell DA. Site-specific incorporation of tryptophan analogues into recombinant proteins in bacterial cells. *J. Am. Chem. Soc.* 2007; 129:10431–10437. [PubMed: 17685515]
- [77]. Lepthien S, Hoessl MG, Merkel L, Budisa N. Azatryptophans endow proteins with intrinsic blue fluorescence. *P. Natl. Acad. Sci. U.S.A.* 2008; 105:16095–16100.
- [78]. Zhang KC, Diehl MR, Tirrell DA. Artificial polypeptide scaffold for protein immobilization. *J. Am. Chem. Soc.* 2005; 127:10136–10137. [PubMed: 16028902]
- [79]. Nowatzki PJ, Franck C, Maskarinec SA, Ravichandran G, Tirrell DA. Mechanically tunable thin films of photosensitive artificial proteins: Preparation and characterization by nanoindentation. *Macromolecules.* 2008; 41:1839–1845.
- [80]. Deming TJ, Fournier MJ, Mason TL, Tirrell DA. Biosynthetic incorporation and chemical modification of alkene functionality in genetically engineered polymers. *J. Macromol Sci. Pure.* 1997; A34:2143–2150.
- [81]. van Hest JCM, Kiick KL, Tirrell DA. Efficient incorporation of unsaturated methionine analogues into proteins in vivo. *J. Am. Chem. Soc.* 2000; 122:1282–1288.
- [82]. Kiick KL, van Hest JCM, Tirrell DA. Expanding the scope of protein biosynthesis by altering the methionyl-tRNA synthetase activity of a bacterial expression host. *Angew. Chem. Int. Edit.* 2000; 39:2148–2152.
- [83]. Zhang ZW, Wang L, Brock A, Schultz PG. The selective incorporation of alkenes into proteins in *Escherichia coli*. *Angew. Chem. Int. Edit.* 2002; 41:2840–2842.
- [84]. Song W, Wang Y, Qu J, Lin Q. Selective functionalization of a genetically encoded alkene-containing protein via “Photoclick Chemistry” in bacterial cells. *J. Am. Chem. Soc.* 2008; 130:9654–9655. [PubMed: 18593155]
- [85]. Ayyadurai N, Kim SY, Lee SG, Nagasundarapandian S, Hasneen A, Paik HJ, An SSA, Oh E. Biological synthesis of alkyne-terminated telechelic recombinant protein. *Macromol. Res.* 2009; 17:424–429.
- [86]. Nguyen DP, Lusic H, Neumann H, Kapadnis PB, Deiters A, Chin JW. Genetic encoding and labeling of aliphatic azides and alkynes in recombinant proteins via a pyrrolysyl-tRNA synthetase/tRNA<sub>CUA</sub> pair and click chemistry. *J. Am. Chem. Soc.* 2009; 131:8720–8721. [PubMed: 19514718]
- [87]. Teeuwen RLM, van Berkel SS, van Dulmen THH, Schoffelen S, Meeuwissen SA, Zuilhof H, Wolf F.A. de, van Hest JCM. “Clickable” elastins: elastin-like polypeptides functionalized with azide or alkyne groups. *Chem. Commun.* 2009; 27:4022–4024.
- [88]. Kiick KL, Saxon E, Tirrell DA, Bertozzi CR. Incorporation of azides into recombinant proteins for chemoselective modification by the Staudinger ligation. *P. Natl. Acad. Sci. U.S.A.* 2002; 99:19–24.
- [89]. Ohno S, Matsui M, Yokogawa T, Nakamura M, Hosoya T, Hiramatsu T, Suzuki M, Hayashi N, Nishikawa K. Site-selective post-translational modification of proteins using an unnatural amino acid, 3-azidotyrosine. *J. Biochem.* 2007; 141:335–343. [PubMed: 17202192]
- [90]. Tanrikulu IC, Schmitt E, Mechulam Y, Goddard WA, Tirrell DA. Discovery of *Escherichia coli* methionyl-tRNA synthetase mutants for efficient labeling of proteins with azidonorleucine in vivo. *P. Natl. Acad. Sci. U.S.A.* 2009; 106:15285–15290.



- [91]. Datta D, Wang P, Carrico IS, Mayo SL, Tirrell DA. A designed phenylalanyl-tRNA synthetase variant allows efficient in vivo incorporation of aryl ketone functionality into proteins. *J. Am. Chem. Soc.* 2002; 124:5652–5653. [PubMed: 12010034]
- [92]. Tang Y, Wang P, Van Deventer JA, Link AJ, Tirrell DA. Introduction of an aliphatic ketone into recombinant proteins in a bacterial strain that overexpresses an editing-impaired leucyl-tRNA synthetase. *Chembiochem.* 2009; 10:2188–2190. [PubMed: 19670197]
- [93]. Tsutsumi Y, Onda M, Nagata S, Lee B, Kreitman RJ, Pastan I. Site-specific chemical modification with polyethylene glycol of recombinant immunotoxin anti-Tac(Fv)-PE38 (LMB-2) improves antitumor activity and reduces animal toxicity and immunogenicity. *P. Natl. Acad. Sci. U.S.A.* 2000; 97:8548–8553.
- [94]. Hinds KD, Kim SW. Effects of PEG conjugation on insulin properties. *Adv. Drug Deliv. Rev.* 2002; 54:505–530. [PubMed: 12052712]
- [95]. Wang YS, Youngster S, Grace M, Bausch J, Bordens R, Wyss DF. Structural and biological characterization of PEGylated recombinant interferon alpha-2b and its therapeutic implications. *Adv. Drug Deliv. Rev.* 2002; 54:547–570. [PubMed: 12052714]
- [96]. Caliceti P, Veronese FM. Pharmacokinetic and biodistribution properties of poly(ethylene glycol)-protein conjugates. *Adv. Drug Deliv. Rev.* 2003; 55:1261–1277. [PubMed: 14499706]
- [97]. Hermeling S, Crommelin DJA, Schellekens H, Jiskoot W. Structure immunogenicity relationships of therapeutic proteins. *Pharm. Res.* 2004; 21:897–903. [PubMed: 15212151]
- [98]. Frokjaer S, Otzen DE. Protein drug stability: A formulation challenge. *Nat. Rev. Drug Discov.* 2005; 4:298–306. [PubMed: 15803194]
- [99]. Wang Y, Kiick KL. Monodisperse protein-based glycopolymers via a combined biosynthetic and chemical approach. *J. Am. Chem. Soc.* 2005; 127:16392–16393. [PubMed: 16305215]
- [100]. Liu S, Kiick KL. Architecture effects on the binding of cholera toxin by helical glycopolypeptides. *Macromolecules.* 2008; 41:764–772. [PubMed: 19214239]
- [101]. Pace CN, Scholtz JM. A helix propensity scale based on experimental studies of peptides and proteins. *Biophys. J.* 1998; 75:422–427. [PubMed: 9649402]
- [102]. Farmer RS, Top A, Argust LM, Liu S, Kiick KL. Evaluation of conformation and association behavior of multivalent alanine-rich polypeptides. *Pharm. Res.* 2008; 25:700–708. [PubMed: 17674161]
- [103]. Goeden-Wood NL, Conticello VP, Muller SJ, Keasling JD. Improved assembly of multimeric genes for the biosynthetic production of protein polymers. *Biomacromolecules.* 2002; 3:874–879. [PubMed: 12099837]
- [104]. Doig AJ. Recent advances in helix-coil theory. *Biophys. Chem.* 2002; 101:281–293. [PubMed: 12488008]
- [105]. Scholtz JM, Qian H, Robbins VH, Baldwin RL. The energetics of ion-pair and hydrogen-bonding interactions in a helical peptide. *Biochemistry.* 1993; 32:9668–9676. [PubMed: 8373771]
- [106]. Israelachvili, JN. *Intermolecular and Surface Forces: With Applications to Colloidal and Biological Systems.* Academic; New York: 1992.
- [107]. Top A, Kiick KL, Roberts CJ. Modulation of self-association and subsequent fibril formation in an alanine-rich helical polypeptide. *Biomacromolecules.* 2008; 9:1595–1603. [PubMed: 18452331]
- [108]. Kiessling LL, Pohl NL. Strength in numbers: Non-natural polyvalent carbohydrate derivatives. *Chem. Biol.* 1996; 3:71–77. [PubMed: 8807830]
- [109]. Mammen M, Choi SK, Whitesides GM. Polyvalent interactions in biological systems: Implications for design and use of multivalent ligands and inhibitors. *Angew. Chem. Int. Edit.* 1998; 37:2755–2794.
- [110]. Kitov PI, Sadowska JM, Mulvey G, Armstrong GD, Ling H, Pannu NS, Read RJ, Bundle DR. Shiga-like toxins are neutralized by tailored multivalent carbohydrate ligands. *Nature.* 2000; 403:669–672. [PubMed: 10688205]
- [111]. Kiessling LL, Gestwicki JE, Strong LE. Synthetic multivalent ligands as probes of signal transduction. *Angew. Chem. Int. Edit.* 2006; 45:2348–2368.

- [112]. Bouchard M, Zurdo J, Nettleton EJ, Dobson CM, Robinson CV. Formation of insulin amyloid fibrils followed by FTIR simultaneously with CD and electron microscopy. *Protein Sci.* 2000; 9:1960–1967. [PubMed: 11106169]
- [113]. Ramirez-Alvarado M, Merkel JS, Regan L. A systematic exploration of the influence of the protein stability on amyloid fibril formation in vitro. *P. Natl. Acad. Sci. U.S.A.* 2000; 97:8979–8984.
- [114]. Srisailam S, Wang HM, Kumar TKS, Rajalingam D, Sivaraja V, Sheu HS, Chang YC, Yu C. Amyloid-like fibril formation in an all  $\beta$ -barrel protein involves the formation of partially structured intermediate(s). *J. Biol. Chem.* 2002; 277:19027–19036. [PubMed: 11877422]
- [115]. Fandrich M, Forge V, Buder K, Kittler M, Dobson CM, Diekmann S. Myoglobin forms amyloid fibrils by association of unfolded polypeptide segments. *P. Natl. Acad. Sci. U.S.A.* 2003; 100:15463–15468.
- [116]. Arnaudov LN, de Vries R. Thermally induced fibrillar aggregation of hen egg white lysozyme. *Biophys. J.* 2005; 88:515–526. [PubMed: 15489299]
- [117]. Sharma N, Top A, Kiick KL, Pochan DJ. One-dimensional gold nanoparticle arrays by electrostatically directed organization using polypeptide self-assembly. *Angew. Chem. Int. Edit.* 2009; 48:7078–7082.
- [118]. Eanes ED, Glenner GG. X-ray diffraction studies on amyloid filaments. *J. Histochem. Cytochem.* 1968; 16:673–677. [PubMed: 5723775]
- [119]. Sunde M, Serpell LC, Bartlam M, Fraser PE, Pepys MB, Blake CCF. Common core structure of amyloid fibrils by synchrotron X-ray diffraction. *J. Mol. Biol.* 1997; 273:729–739. [PubMed: 9356260]
- [120]. Jackson M, Mantsch HH. The use and misuse of FTIR spectroscopy in the determination of protein-structure. *Crit. Rev. Biochem. Mol.* 1995; 30:95–120.
- [121]. Sunde M, Blake CCF. From the globular to the fibrous state: Protein structure and structural conversion in amyloid formation. *Q. Rev. Biophys.* 1998; 31:1–39. [PubMed: 9717197]
- [122]. Nilsson MR. Techniques to study amyloid fibril formation in vitro. *Methods.* 2004; 34:151–160. [PubMed: 15283924]
- [123]. Turkevich J, Stevenson PC, Hillier J. A study of the nucleation and growth processes in the synthesis of colloidal gold. *Discuss. Faraday Soc.* 1951; 11:55–65.
- [124]. Burkoth TS, Benzinger TLS, Jones DNM, Hallenga K, Meredith SC, Lynn DG. C-terminal PEG blocks the irreversible step in  $\beta$ -amyloid(10-35) fibrillogenesis. *J. Am. Chem. Soc.* 1998; 120:7655–7656.
- [125]. Burkoth TS, Benzinger TLS, Urban V, Lynn DG, Meredith SC, Thiyagarajan P. Self-assembly of A $\beta$  ((10-35))-PEG block copolymer fibrils. *J. Am. Chem. Soc.* 1999; 121:7429–7430.
- [126]. Bae Y, Fukushima S, Harada A, Kataoka K. Design of environment-sensitive supramolecular assemblies for intracellular drug delivery: Polymeric micelles that are responsive to intracellular pH change. *Angew. Chem. Int. Edit.* 2003; 42:4640–4643.
- [127]. Bae Y, Jang WD, Nishiyama N, Fukushima S, Kataoka K. Multifunctional polymeric micelles with folate-mediated cancer cell targeting and pH-triggered drug releasing properties for active intracellular drug delivery. *Mol. Biosyst.* 2005; 1:242–250. [PubMed: 16880988]
- [128]. Bae Y, Nishiyama N, Kataoka K. In vivo antitumor activity of the folate conjugated pH-Sensitive polymeric micelle selectively releasing adriamycin in the intracellular acidic compartments. *Bioconjugate Chem.* 2007; 18:1131–1139.
- [129]. Allen C, Maysinger D, Eisenberg A. Nano-engineering block copolymer aggregates for drug delivery. *Colloid. Surface. B.* 1999; 16:3–27.
- [130]. Cai SS, Vijayan K, Cheng D, Lima EM, Discher DE. Micelles of different morphologies - Advantages of worm-like filomicelles of PEO-PCL in paclitaxel delivery. *Pharm. Res.* 2007; 24:2099–2109. [PubMed: 17564817]
- [131]. Geng Y, Dalhaimer P, Cai SS, Tsai R, Tewari M, Minko T, Discher DE. Shape effects of filaments versus spherical particles in flow and drug delivery. *Nat. Nanotechnol.* 2007; 2:249–255. [PubMed: 18654271]

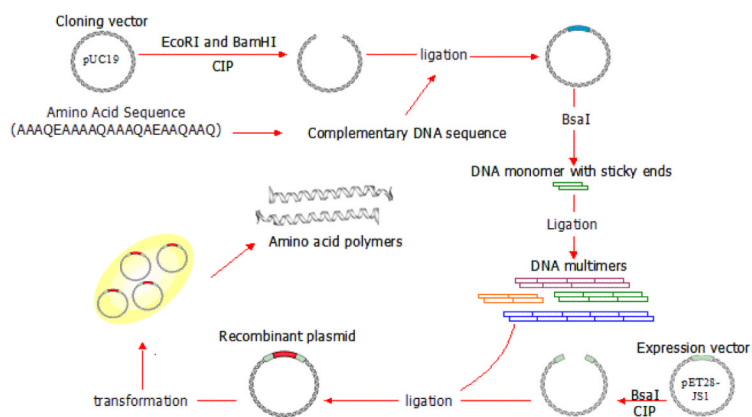


**Figure 1.** Simplified gene construction scheme for a representative polypeptide. Figure

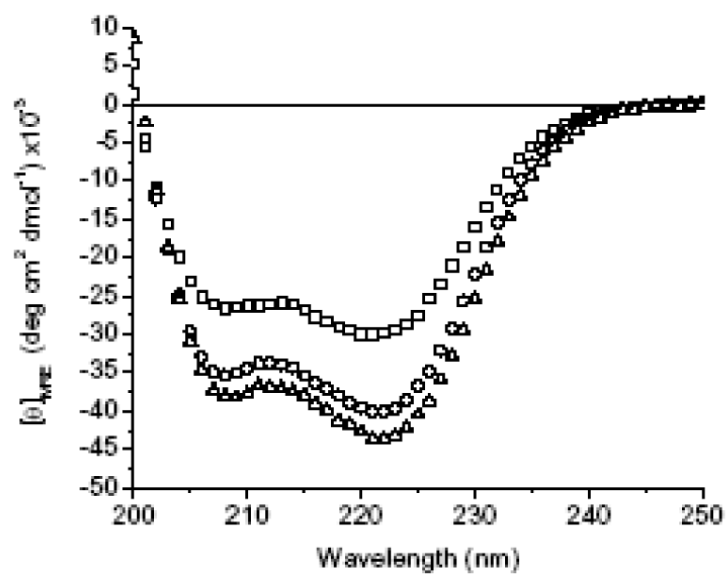


**Figure 2.** CD spectra of 17-H-3 (open squares), 17-H-6 (open circles), and 35-H-6 (open triangles) in PBS buffer at pH 7.4 at 5 °C. Reproduced with permission from [102]. Copyright (2008) Springer.

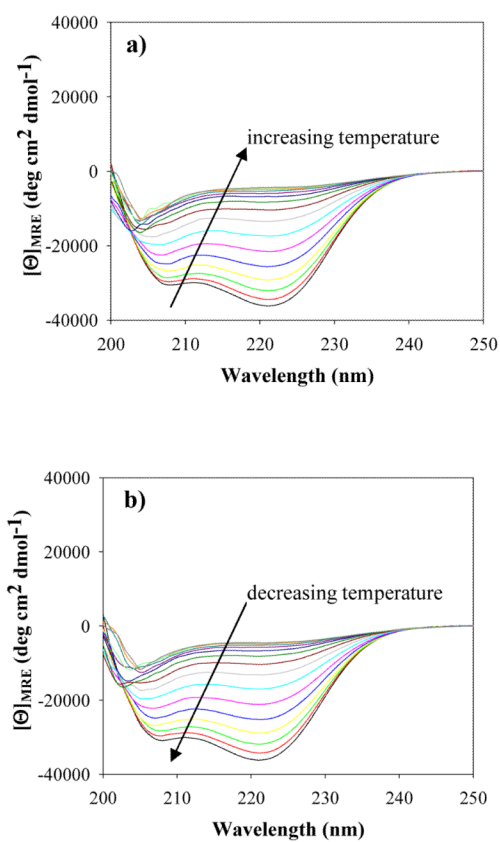


**Figure 3.** CD spectra of 17-H-6 during a) unfolding and b) refolding in PBS buffer at pH 7.4. Reproduced with permission from [107]. Copyright (2008) American Chemical Society.



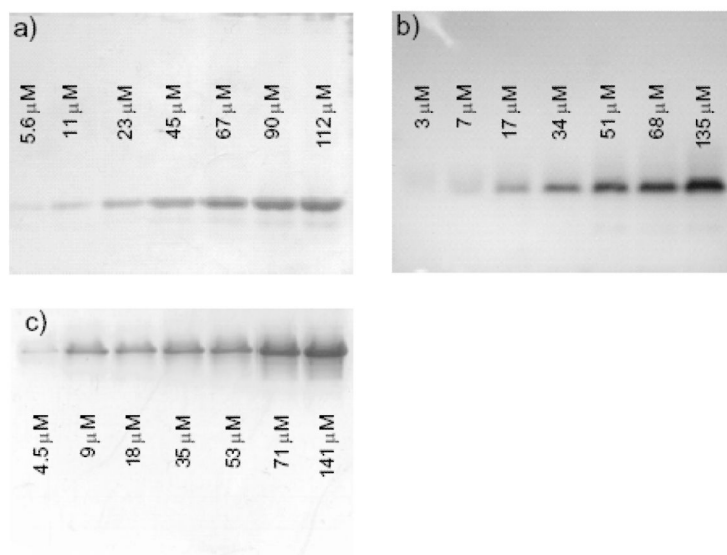


**Figure 4.** Non-denaturing gel electrophoresis of a) 17-H-3, b) 17-H-6, and c) 35-H-6 at various concentrations. Reproduced with permission from [102]. Copyright (2008) Springer.

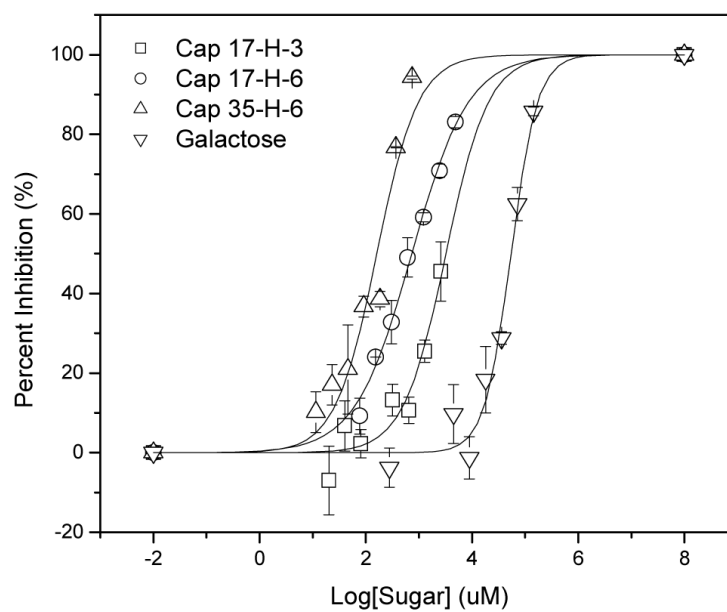


**Figure 5.** CT B<sub>5</sub> inhibition curves of the glycopolypeptides and galactose. Reproduced with permission from [100]. Copyright (2008) American Chemical Society.

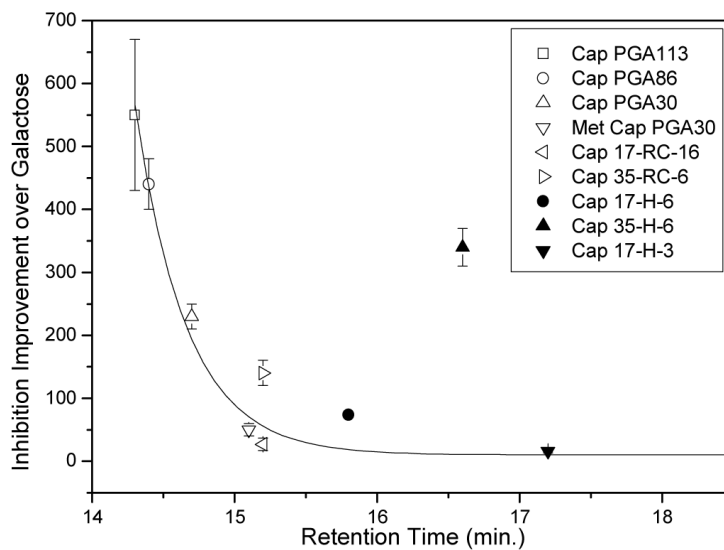


**Figure 6.** Correlation of inhibition improvement and retention time in GPC for randomcoil glycopolyptides (open) [8] and  $\alpha$ -helical glycopolyptides (solid). Reproduced with permission from [100]. Copyright (2008) American Chemical Society.

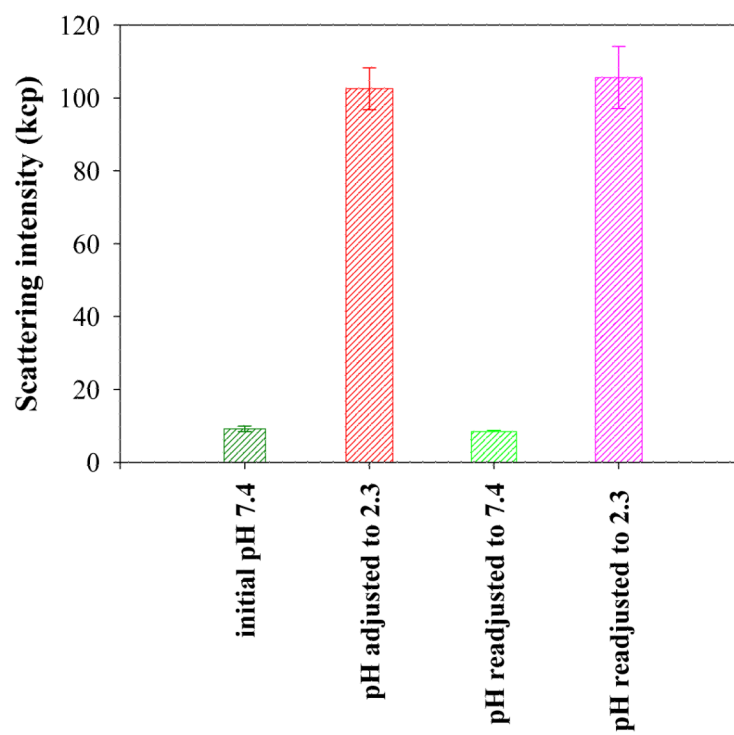


**Figure 7.**  
Change in the scattering intensity of 17-H-6 solution as a function of pH.

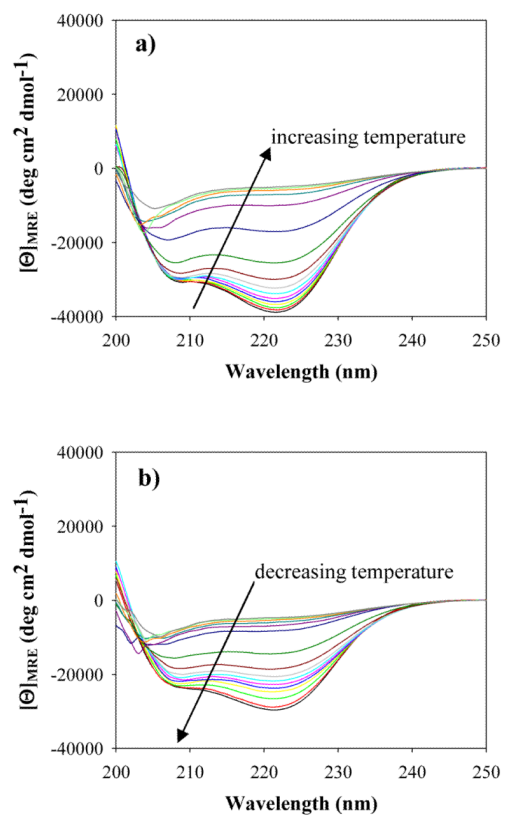


**Figure 8.** CD spectra of 17-H-6 during a) unfolding and b) refolding of 17-H-6 at pH 2.3 buffer. Reproduced with permission from [107]. Copyright (2008) American Chemical Society.



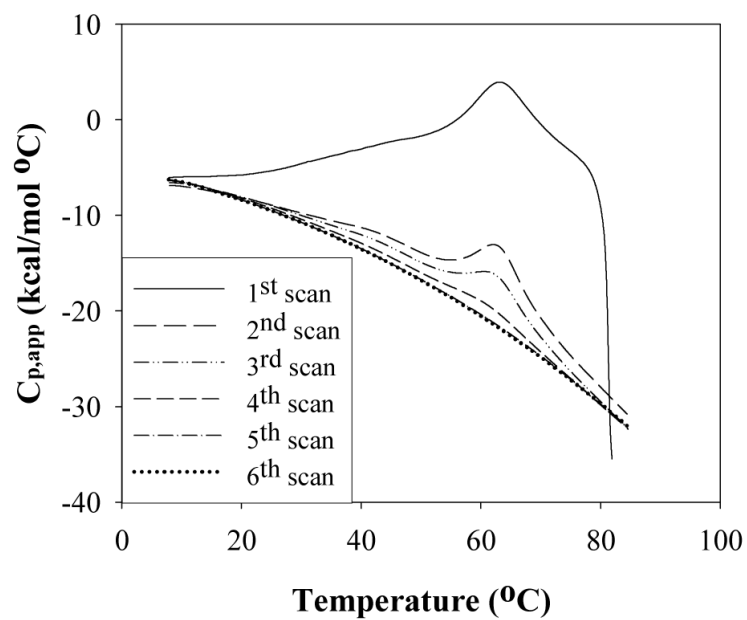


**Figure 9.** Consecutive DSC scans of 17-H-6 in pH 2.3 buffer. Reproduced with permission from [107]. Copyright (2008) American Chemical Society.

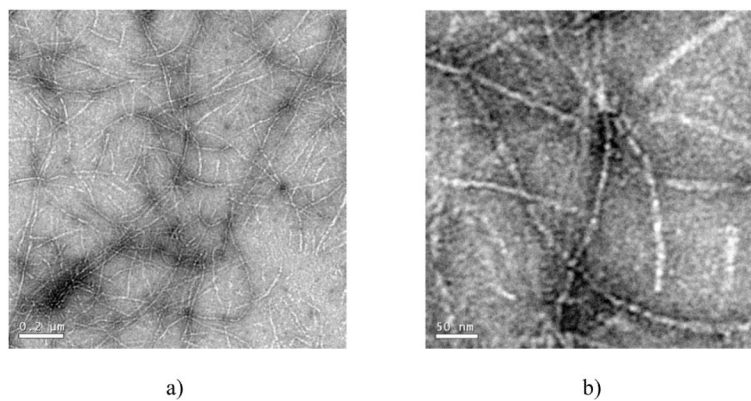


**Figure 10.** TEM pictures of 100  $\mu\text{M}$  of 17-H-6 in pH 2.3 buffer annealed at 80  $^{\circ}\text{C}$  for 18 hrs. Scale bars: a) 200 nm b) 50 nm. Reproduced with permission from [107]. Copyright (2008) American Chemical Society.

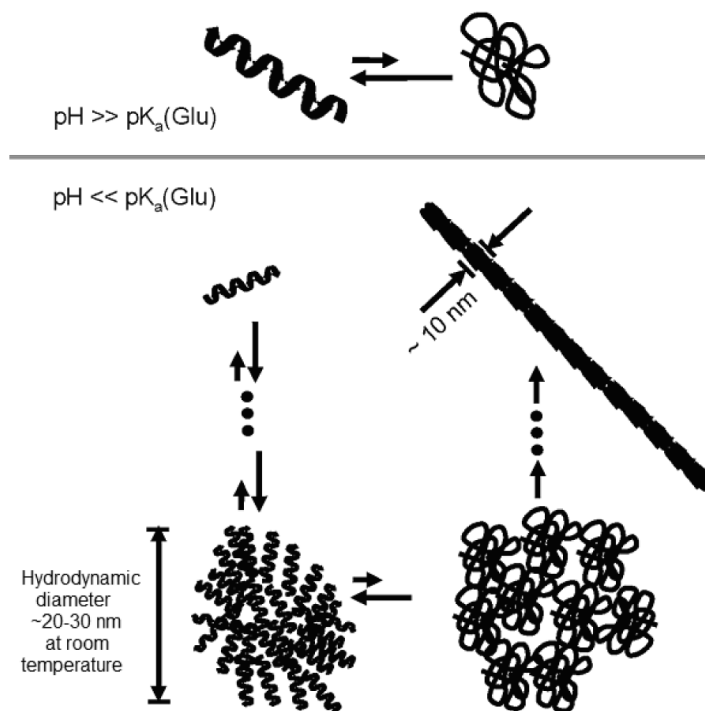


**Figure 11.** Summary of the conformation and aggregation behavior of 17-H-6 as a function of pH and temperature. Reproduced with permission from [107]. Copyright (2008) American Chemical Society.

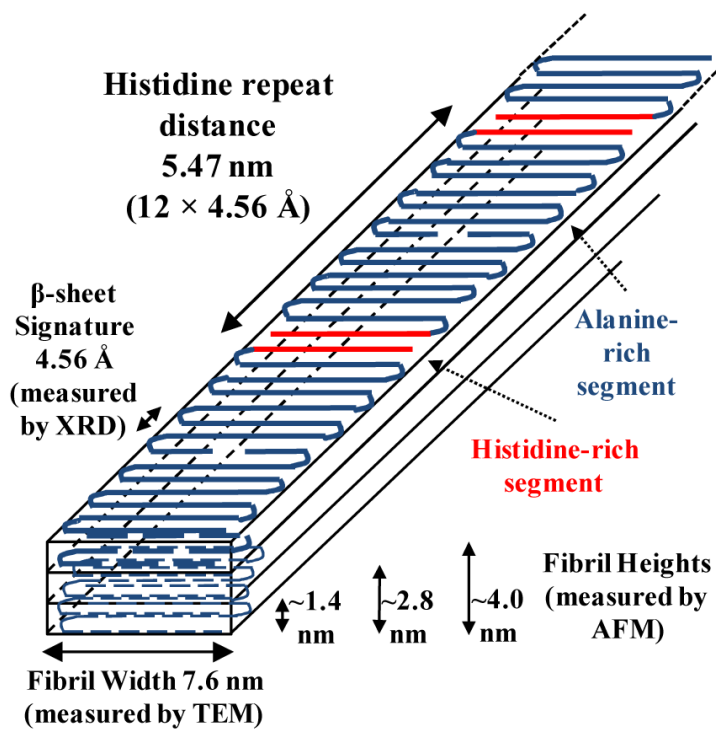


**Figure 12.** Suggested fibril assembly model of 17-H-6. Reproduced with permission from [117]. Copyright (2009) Wiley.

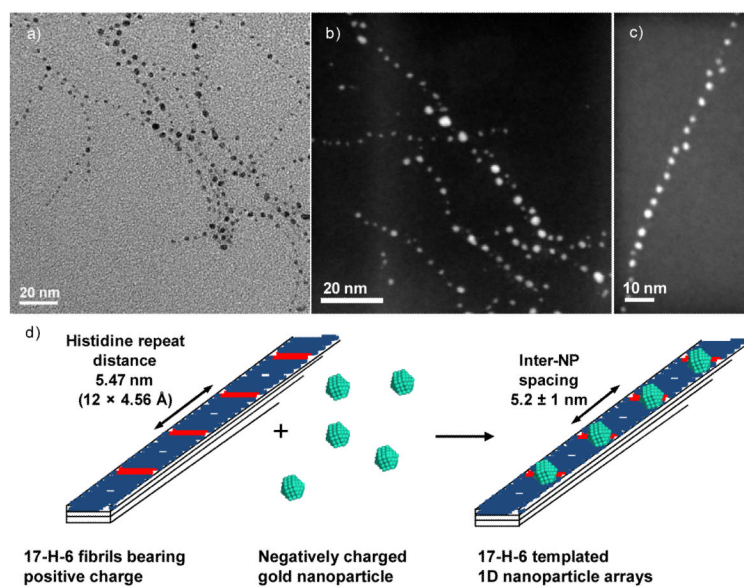


**Figure 13.**

a) BF TEM image of 17H6 templated 1D gold nanoparticle arrays; b) HAADF-STEM image showing high fidelity of the 2 nm gold nanoparticles to the 17H6 fibrils; c) HAADF STEM image showing controlled axial nanoparticle positioning with  $5.2 \pm 1$  nm inter-particle spacing; d) Schematic showing mechanism for electrostatic assembly of negatively charged gold nanoparticles on positively charged histidine patches in 17-H-6 fibrils. Reproduced with permission from [117]. Copyright (2009) Wiley.

**Table 1**

Summary of the helical polypeptides [7,102]

Notation <sup>*</sup>	Sequence <sup>**</sup>	MW (Da)	# of E	E Spacing (Å)
17-H-3	[AAAEAAAAQAAAEAAQAAQ] <sub>3</sub>	8875	6	17
17-H-6	[AAAEAAAAQAAAEAAQAAQ] <sub>6</sub>	14770	12	17
35-H-6	[AAAEAAQAAAEAAQAAQ] <sub>6</sub>	14159	6	35

\* The polypeptides were named according to notation, XHY, where X denotes the distance between E residues, H emphasizes backbone is helical, and Y is the number of repeating unit [102]

\*\* All the sequences contain N-terminal histidine tag, MGH10S2GHIHM, and all experiments were carried out on polypeptides containing the fusion tag, unless otherwise stated.